Buckling of Cylindrical Shells with Intermittently Attached Stiffeners

TSAI-CHEN SOONG*
The Boeing Company, Seattle, Wash.

A linear analysis for the general instability of eccentrically stiffened orthotropic cylinders with intermittently attached stiffeners is presented. A buckling determinant is derived as an example for a stiffened orthotropic cylinder under bending and uniform axial loads, with the attachment of stringer-to-skin and frame-to-skin, respectively, assumed to be monolithic and intermittent. An approximate method of including the effect of prematurely buckled skin in instability analyses of stiffened cylinders is suggested. Applied to cylinders with fully attached stiffeners, the analysis shows good correlation with test results on ring-stiffened corrugated cylinders under various axial loads and ring-and-stringer stiffened cylinders with prematurely buckled skin under bending loads. For cylinders with intermittently attached stiffeners, a correlation was obtained with test results on a 128-in.-radius cylinder specimen made specifically to study the effect of shear-ties on the buckling strength of transport airplane fuselages with prematurely buckled skins. The error in predicting the improved buckling strength of the cylinder due to the addition of shear-ties on the floating-type frames is found to be within 1.8%.

Nomenclature

A_r, A'_r = cross-sectional area of frame with and without shear-tie
A_s = cross-sectional area of stringer
D = bending stiffness of isotropic plate, $Et^3/[12(1-\nu^2)]$
D_x, D_y, D_{xy} = bending and twisting stiffnesses of orthotropic plate
E, G = Young's modulus and shear modulus, respectively
E_x, E_y, G_{xy} = extensional and shear stiffnesses of orthotropic plate
I_{os}, I_{or} = moment of inertia of stringer and of attached frame, respectively, about midsurface of the shell
I'_r = moment of inertia of free frame about its own neutral axis
J_r, J'_r = St. Venant torsional constant for frame with and without shear-tie
J_s = St. Venant torsional constant for stringer
L = nondimensional length of cylinder, true length/R
L_y = nondimensional half-circumference of the cylinder section
$\bar{N}_x, \bar{N}_y, \bar{N}_{xy}$ = applied compressive loads and shear load, force/unit length
R = radius of cylinder (Fig. 2)
R_r = radius of free frame (Fig. 2)
$W_e, \bar{W}_s, \bar{W}_r$ = effective width [Eqs. (A1), (B15), and (B16)]
d = stringer spacing
h = nondimensional distance of neutral axis
$\bar{k}_1, \bar{k}_2$ = const [Eq. (A1)], $\bar{k}_1 \cong \pi^2/[3(1-\nu^2)]$
n, m = numbers of full circumferential waves and axial half-waves
$\bar{m}$ = $m\pi/L$
q_s = effective width parameter [Eq. (B17)]
t = thickness of skin
u, v, w = nondimensional axial, circumferential, and radial inward displacements at the median surface of the cylinder
$\bar{v}, \bar{w}$ = nondimensional displacements at the neutral axis of the free frame (Fig. 2)
x, y, z = nondimensional rectangular coordinates
$\bar{z}$ = eccentric distance of stiffeners measured from center of gravity of sections; positive if stiffeners are internal
β = angle in radians; associated with partially effective skin, Eq. (A4)
ϵ = direct strain, Eq. (10)
μ_x, μ_y = Poisson's ratios for bending of orthotropic plate
μ'_x, μ'_y = Poisson's ratios for extension of orthotropic plate
ν = Poisson's ratio for isotropic plate
σ = direct stress, positive for compression
σ_0 = compressive stress at the crown, Eq. (A2)

Subscripts

i = station number of stringers and shear-tie locations
j = station numbering of frames
r, s = properties of frames and stringers, respectively
x, y = axial and circumferential coordinates

Received June 9, 1969; revision received October 10, 1969. The author acknowledges the help of C. Li of The Boeing Company in the programing and in computation of the results. He also acknowledges R. E. Miller Jr. and P. J. Harradine for valuable discussions.

* Senior Specialist Structures Staff, Commercial Airplane Group.

I. Introduction

IN the literature of the general instability analysis of stiffened shells, the stiffener-to-skin attachment has always been treated as monolithic and continuous. The assumption regarding sheet metal connections as monolithic (usually means machined, bonded, seam welded, etc.) is generally true and has been extended in instability analyses of stiffened cylinders to include discrete fastenings, such as riveting or spot welding. Tests by Peterson and Anderson[1] and by Anderson[2] substantiated this idealization for riveted fastenings on stiffened cylinders.

However, the second assumption, that stiffeners are continuously attached to the skin for their entire length, is not always true in real structures. An important case is the so-called floating-type fuselage construction in which the stringers (longitudinal stiffeners) are continuously attached to the skin but the ring-type frames are intermittently fastened (only to stringers). Figure 1 shows a typical idealized floating connection. A common practice to improve the rigidity of such structures, often required in critical portions of the fuselage, is to secure the skin to the frames by means of a piece of sheet metal (called a shear-tie) riveted across the spacing between two stringers (called a bay). The effect of the addition of such irregular reinforcements on the general instability behavior of floating-type stiffened cylinders is

usually estimated from designers' experience; there are no theoretical studies and no test data available in the literature.

The present study examines the general instability of stiffened circular cylinders whose frames are attached to the skin in a pointwise and piecewise manner. A case with bending load is studied in detail. Donnell-type linear strain-displacement relationships and the direct method of minimization of the total potential are used in the analysis. The adequacy of the linear theory, which disregards geometric imperfections and prebuckling deformation in the treatment of the general instability problems of stiffened cylinders, has been studied frequently, and reasonably good test correlations have been obtained by a number of investigators.[3-11]

In the present derivation, discreteness of stiffeners is idealized mathematically by use of the Dirac delta function.[4] Stringers and continuously attached frames are treated as eccentric beam elements integrally supported by the skin.[3,12] The portion of the frame not connected to the skin is considered as a beam with end constraints that is geometrically compatible with the skin at the two points of contact.

A buckling determinant is derived for a ring-and-stringer stiffened orthotropic cylinder with simply supported ends. Methods that include the effect of prematurely buckled skin in the analysis are suggested. Predicted results are correlated with test data and compared with the analyses from other theories. The theoretical derivations, which follow the usual strain energy approach, are presented in subsequent sections.

II. Total Potential of the Stiffened Cylinder

For a shell with orthotropic skin, the increment of the elastic strain energy corresponding to the median surface stresses and bending can be written as[12]

$$U_c = \frac{1}{2} R^2 \int_0^{2\pi} \int_0^L [A_1(u_{,x})^2 + 2A_2 u_{,x}(v_{,y} - w) + A_3(v_{,x} + u_{,y})^2 + A_4(v_{,y} - w)^2 + A_5(w_{,xx})^2 + 2A_6 w_{,xx} w_{,yy} + 2A_7(w_{,xy})^2 + A_8(w_{,yy})^2] dx dy \quad (1)$$

where the median surface displacements u, v, and w and the coordinates x and y are nondimensional quantities (the true quantity divided by R). (A coordinate subscript preceded by a comma denotes partial differentiation with respect to the subscript.) The coefficients are defined as

$$\begin{aligned} A_1 &= E_x/(1 - \mu'_x\mu'_y) & A_2 &= \tfrac{1}{2}(E_x\mu'_y + E_y\mu'_x)/(1 - \mu'_x\mu'_y) \\ A_3 &= G_{xy} & A_4 &= E_y/(1 - \mu'_x\mu'_y) \\ A_5 &= D_x/[R^2(1 - \mu_x\mu_y)] & A_6 &= (D_x\mu_y + D_y\mu_x)/[2R^2(1 - (\mu_x\mu_y)] \\ A_7 &= D_{xy}/R^2 & A_8 &= D_y/[R^2(1 - \mu_x\mu_y)] \end{aligned} \quad (2)$$

where the orthotropic constants E_x, D_x, etc. are the same as those defined by Stein and Mayers.[13] Definitions of the notations used are collected in the Nomenclature.

For simplicity but without loss of generality, it is assumed that the stringers are connected to the skin in a monolithic manner, whereas the frames are intermittently attached.

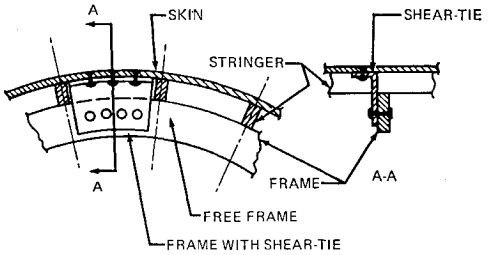

Fig. 1 Idealized floating-type construction with intermittently shear-tied frame.

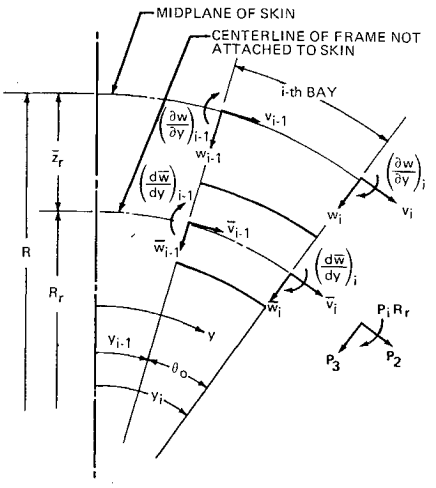

Fig. 2 Displacements and forces on the end points of a portion of frame not attached to the skin.

The strain energy of stringers in terms of midplane deformation of the skin can be approximately expressed as[12]

$$U_s = \frac{1}{2} R \sum_{i=1}^{2N} \delta(y - y_i) \int_0^L \left[\int_{A_s} E_s(u_{,x} - z w_{,xx})^2 \, dA_s + (G_s J_s/R^2)(w_{,xy})^2 \right] dx \quad (3)$$

where y_i is the coordinate of the ith stringer and $2N$ is the total number of stringers. The Dirac delta function $\delta(y - y_i)$ is defined as usual, that is, it is equal to unity when $y = y_i$ and vanishes when $y \neq y_i$. The use of the Dirac function to describe the discrete nature of the stiffeners is adequate only when the width of the stiffener is small compared with the spacing.[4]

After integration, Eq. (3) becomes

$$U_s = \frac{1}{2} R^2 \sum_{i=1}^{2N} \delta(y - y_i) \int_0^L [A_9(u_{,x})^2 - 2A_{10} u_{,x} w_{,xx} + A_{11}(w_{,xx})^2 + A_{12}(w_{,xy})^2] dx \quad (4)$$

where the stiffnesses of the stringer are included in the constants

$$\begin{aligned} A_9 &= E_s A_s/R & A_{10} &= E_s A_s \bar{z}_s/R^2 \\ A_{11} &= E_s I_{os}/R^3 & A_{12} &= G_s J_s/R^3 \end{aligned} \quad (5)$$

For the portion of the frame located at $x = x_j$ and continuously attached to the skin of the shell between $y = y_{i-1}$ and y_i, the strain energy expression is similar to that of the stringer, as shown in Eq. (4), except that frames run in the y direction and possess a constant curvature of $1/R$:

$$\Delta U_r = \frac{1}{2} R^2 \delta(x - x_j) \int_{y_{i-1}}^{y_i} [B_1(v_{,y} - w)^2 - 2B_2(v_{,y} - w) w_{,yy} + B_3(w_{,yy})^2 + B_4(w_{,xy})^2] dy \quad (6)$$

where

$$\begin{aligned} B_1 &= E_r A_r/R & B_2 &= E_r A_r \bar{z}_r/R^2 \\ B_3 &= E_r I_{or}/R^3 & B_4 &= G_r J_r/R^3 \end{aligned} \quad (7)$$

If the portion of the frame between y_{i-1} and y_i is not attached to the skin, then its strain energy depends on the slopes and displacements at the two end points y_{i-1} and y_i of the frame. Let $\bar{v}$ and $\bar{w}$ be the nondimensional displacements at the neutral axis of the free frame and A'_r, I'_r, and J'_r be the sectional properties of the frame with respect to the center of gravity of the section. Then the strain energy of the free frame located at $x = x_j$ and $y_{i-1} \leq y \leq y_i$ can be

written approximately as

$$\Delta U_r = \frac{1}{2} R_r \delta(x - x_j) \left\{ \int_{y_{i-1}}^{y_i} \left[A'_r E_r (R/R_r)^2 \left(\frac{d\bar{v}}{dy} - \bar{w} \right)^2 + (E_r I'_r R^2 / R_r^4) \left(\frac{d^2\bar{w}}{dy^2} \right)^2 \right] dy + G_r J'_r \left[\frac{(w,_x)_i - (w,_x)_{i-1}}{R_r (y_i - y_{i-1})} \right]^2 \times (y_i - y_{i-1}) \right\} \quad (8)$$

where R_r is the radius of the frame. Figure 2 illustrates the notation used for a portion of frame not attached to the skin. The derivation of the right-hand side of Eq. (8) in terms of the skin deformation, w, v, and $w,_y$, at the end points $y = y_{i-1}$ and y_i of $x = x_j$ follows.

The differential equations of equilibrium of a portion of the frame with end loads P_1, P_2, and P_3 acting at y_i, as shown in Fig. 2, can be shown as

$$\frac{d^2\bar{w}}{dy^2} = \frac{R_r^3}{RE_r I'_r} \{ P_1 + P_3 \sin(y_i - y) + P_2 [1 - \cos(y_i - y)] \} \quad (9)$$

$$\frac{d\bar{v}}{dy} - \bar{w} = \epsilon_y = \frac{R_r}{RA'_r E_r} [P_2 \cos(y_i - y) - P_3 \sin(y_i - y)] \quad (10)$$

The three integration constants of Eqs. (9) and (10) can be determined exactly by assuming that the frame displace ments $\bar{u}$, $\bar{w}$, and rotation $d\bar{w}/dy$ at one end, say y_{i-1}, are known. In addition, assuming that the frame remains perpendicular to the skin at the points of contact and the relative translation between w and $\bar{w}$ is being neglected, the following displacement relationships between the frame and the skin exist at y_{i-1} and y_i:

$$\bar{v} = v - (\bar{z}_r/R)(w,_y), \qquad \bar{w} = w, \qquad d\bar{w}/dy = w,_y \quad (11)$$

Thus, after integration and substitution of integration constants, Eqs. (9) and (10) become

$$\bar{w} = K_1 \{ \tfrac{1}{2} P_1 (y - y_{i-1})^2 + P_3 [\sin\theta_0 - \sin(y_{i-1} + \theta_0 - y) - \cos\theta_0 (y - y_{i-1})] + P_2 [\cos(y_{i-1} + \theta_0 - y) - \cos\theta_0 - \sin\theta_0 (y - y_{i-1}) + \tfrac{1}{2}(y - y_{i-1})^2] \} + (w,_y)_{i-1} (R_r/R)(y - y_{i-1}) + w_{i-1} \quad (12)$$

$$\bar{v} = K_1 \{ \tfrac{1}{6} P_1 (y - y_{i-1})^3 + P_3 [-\cos(y_{i-1} + \theta_0 - y) - \tfrac{1}{2}\cos\theta_0 (y - y_{i-1})^2 + \sin\theta_0 (y - y_{i-1}) + \cos\theta_0] + P_2 [\tfrac{1}{6}(y - y_{i-1})^3 - \sin(y_{i-1} + \theta_0 - y) - \tfrac{1}{2}\sin\theta_0 (y - y_{i-1})^2 - \cos\theta_0 (y - y_{i-1}) + \sin\theta_0] \} + K_2 \{ P_3 [\cos\theta_0 - \cos(y_i - y)] + P_2 [\sin\theta_0 - \sin(y_{i-1} + \theta_0 - y)] \} + (w,_y)_{i-1} (R_r/2R)(y - y_{i-1})^2 + w_{i-1}(y - y_{i-1}) + v_{i-1} - (w,_y)_{i-1} (\bar{z}_r/R) \quad (13)$$

where the subscript $i - 1$ indicates the value of a quantity taken at y_{i-1}, and

$$\theta_0 = y_i - y_{i-1}, \qquad K_1 = R_r^3/RE_r I'_r, \qquad K_2 = R_r/RA'_r E_r, \qquad K_3 = G_r J'_r/RR_r \quad (14)$$

The last constant K_3 will appear in Eq. (16). Equations (12) and (13) are the solutions of Eqs. (9) and (10) in terms of the midplane deformation of the skin, w, v, and $w,_y$, tken at y_{i-1}.

Substitution of Eqs. (12) and (13) into Eq. (8) and integration yield

$$\Delta U_r = \tfrac{1}{2} R_r K_1 \delta(x - x_j) \{ G_1 P_1^2 + G_2 P_2^2 + G_3 P_3^2 + 2G_4 P_2 P_3 + 2G_5 P_1 P_2 + 2G_6 P_1 P_3 + G_7 [(w,_x)_i - (w,_x)_{i-1}]^2 \} \quad (15)$$

where

$$G_1 = \theta_0,\ G_2 = \tfrac{3}{2}\theta_0 - 2\sin\theta_0 + \tfrac{1}{4}\sin 2\theta_0 + \tfrac{1}{2}(K_2/K_1)(\theta_0 + \tfrac{1}{2}\sin 2\theta_0),\ G_3 = \tfrac{1}{2}\theta_0 - \tfrac{1}{4}\sin 2\theta_0 + \tfrac{1}{2}(K_2/K_1)(\theta_0 - \tfrac{1}{2}\sin 2\theta_0)$$
$$G_4 = \tfrac{3}{4} - \cos\theta_0 + \tfrac{1}{4}\cos 2\theta_0 - \tfrac{1}{4}(K_2/K_1)(1 - \cos 2\theta_0),\ G_5 = \theta_0 - \sin\theta_0,\ G_6 = 1 - \cos\theta_0,\ G_7 = K_3/(K_1\theta_0) \quad (16)$$

The unknown forces P_1 to P_3 can be obtained in terms of the end displacements through inversion of Eqs. (12) and (13). With the aid of Eq. (11), one obtains the following stiffness matrix relationships:

$$\begin{bmatrix} P_1 \\ P_2 \\ P_3 \end{bmatrix} = K^{-1} \left(\begin{bmatrix} 1 \\ 0 \\ 0 \end{bmatrix} w_i + \begin{bmatrix} -1 \\ -\theta_0 \\ 0 \end{bmatrix} w_{i-1} + \begin{bmatrix} 0 \\ 1 \\ 0 \end{bmatrix} v_i + \begin{bmatrix} 0 \\ -1 \\ 0 \end{bmatrix} v_{i-1} + \begin{bmatrix} 0 \\ -\bar{z}_r/R \\ R_r/R \end{bmatrix} (w,_y)_i + \begin{bmatrix} -\theta_0 R_r/R \\ (-\tfrac{1}{2}\theta_0^2 R_r + \bar{z}_r)/R \\ -R_r/R \end{bmatrix} (w,_y)_{i-1} \right) \quad (17)$$

where K^{-1} is the inverse of a flexibility matrix K defined as

$$K = K_1 \begin{bmatrix} \theta_0^2/2 & 1 + \tfrac{1}{2}\theta_0^2 - \theta_0 \sin\theta_0 - \cos\theta_0 & \sin\theta_0 - \theta_0 \cos\theta_0 \\ \theta_0^3/6 & \tfrac{1}{6}\theta_0^3 - \theta_0 \cos\theta_0 + \sin\theta_0 [1 - \tfrac{1}{2}\theta_0^2 + (K_2/K_1)] & \theta_0 \sin\theta_0 - 1 - (K_2/K_1) + \cos\theta_0 [1 - \tfrac{1}{2}\theta_0^2 + (K_2/K_1)] \\ \theta_0 & \theta_0 - \sin\theta_0 & 1 - \cos\theta_0 \end{bmatrix} \quad (18)$$

By introducing new notation F_{11}, etc., Eq. (17) may be simplified to

$$P_k = F_{k1} w_i + F_{k2} w_{i-1} + F_{k3} v_i + F_{k4} v_{i-1} + F_{k5} (w,_y)_i + F_{k6} (w,_y)_{i-1} \quad k = 1,2,3 \quad (19)$$

Equation (15), together with Eq. (19), is the final expression of the strain energy of a portion of the frame at $x = x_j$ that is not attached to the skin except at the two end points y_{i-1} and y_i; the strain energy is expressed in terms of the displacements of the skin at these two end points.

Finally, the change of the potential of the external loads, which are kept constant during buckling, can be written in the conventional manner:

$$U_{p(\text{skin})} = -\frac{1}{2}R^2\int_0^L\int_0^{2\pi}[\bar{N}_x(w,_x)^2 - 2\bar{N}_{xy}w,_xw,_y + \bar{N}_y(w,_y)^2]dxdy \quad (20)$$

$$U_{p(\text{stringers})} = -\frac{1}{2}R\sum_{i=1}^{2N}\int_0^L(\sigma_{xc} + \sigma_{xb})A_s(w,_x|_{y=y_i})^2dx \quad (21)$$

where $\bar{N}_x$ is the axial compressive load, $\bar{N}_y$ the hoop compression, and $\bar{N}_{xy}$ the torsional load on the skin of the shell, all expressed in force per unit length. The two stresses in Eq. (21), σ_{xc} and σ_{xb}, are stringer stresses due to uniform axial compression and pure bending moment, respectively.

The sum of Eqs. (1, 4, 20, 21, 6, and 15) (the last two equations should be extended to cover all frames) is the change of the total potential of the cylinder because of the buckling deformation. When the total potential is made stationary with respect to an admissible buckling pattern, an eigenvalue problem can be formulated in which the lowest eigenvalue is the buckling load.

III. Symmetric Buckling Modes

As an example, a case for combined bending and uniform axial compressive loads will be analyzed. Since the loading is symmetric, one may stipulate a symmetric buckling pattern that satisfies the classical simply supported end conditions, that is, $w = M_x = N_x = v = 0$ at $x = 0$ and L, as in the following:

$$\left.\begin{aligned} w &= \sum_{m=1}^{\infty}\sum_{n=0}^{\infty}W_{mn}\sin\bar{m}x\cos ny \\ u &= \sum_{m=1}^{\infty}\sum_{n=0}^{\infty}U_{mn}\cos\bar{m}x\cos ny \\ v &= \sum_{m=1}^{\infty}\sum_{n=1}^{\infty}V_{mn}\sin\bar{m}x\sin ny \end{aligned}\right\} \begin{matrix} 0 \le x \le L \\ 0 \le y \le \pi \end{matrix} \quad (22)$$

where W, U, and V with integer subscripts are free constants, n is the circumferential wave number, and $\bar{m}$ is the reduced axial wave number ($\bar{m} = m\pi/L$). The number of Fourier terms required to account accurately for the discontinuities at the junction between free and attached frames may be prohibitive. Fortunately, in the energy approach to structural instability analyses in which the deformation is stipulated, the capability of accurately representing the stress field by the deformation function does not seem to be mandatory in eigenvalue solutions. An example is the "smeared" representation of the stiffeners in closely stiffened cylinders. Reasonably good results have been obtained[1,4,10,11,14] by simple deformation functions, even though the stress field in the vicinity of stiffeners was far more complicated than what the deformation function was able to represent.

With substitution of Eqs. (22) into Eq. (19), the end loads at the free frame characterized by subscripts j and i of x_j and y_i can be written as

$$P_k|_{x=x_j} = \sum_{m=1}^{\infty}\sin\bar{m}x_j\left[\sum_{n=0}^{\infty}W_{mn}Q_k(n,i) + \sum_{n=1}^{\infty}V_{mn}Q_{k+3}(n,i)\right] \quad (23)$$

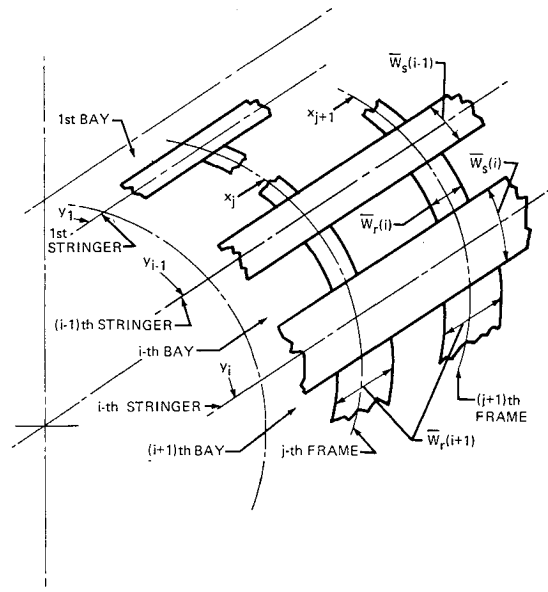

Fig. 3 Effective skin strips attached to stringers and shear-tied frames.

where the Q's are new notations defined as

$$Q_k(n,i) = F_{k1}\cos ny_i + F_{k2}\cos ny_{i-1} - F_{k5}\,n\sin ny_i - F_{k6}\,n\sin ny_{i-1} \quad (24)$$

$$Q_{k+3}(n,i) = F_{k3}\sin ny_i + F_{k4}\,n\sin ny_{i-1}, \qquad k = 1,2,3$$

and F_{11}, F_{12}, etc. are given by Eqs. (17) and (19).

IV. Analysis of Cylinders with Local Skin Buckles

Based on the assumed Fourier series of Eqs. (22), a solution of the buckling problem can be obtained by differentiation of the total potential with respect to coefficients W_{mn}, U_{mn}, and V_{mn} of Eqs. (22), which results in a set of homogeneous simultaneous linear equations. The lowest eigenvalue of the determinant formed by the homogeneous set is the buckling load. The derivations are presented in Appendixes A and B. Certain aspects of cylinders with prematurely buckled skins are discussed below.

It is well known that local buckling of skin considerably reduces the strength of a stiffened cylinder against the general instability failure. To account for the reduced effectiveness of the skin, the ideas of effective skin thickness and effective width[15] were tried in the present study and correlated with test results on ring-and-stringer stiffened cylinders under bending loads.[10,16,17] The correlations were not satisfactory, partly because these equations in their existing form contain no compensation for different rates of reduction in E_x, E_y, G_{xy} and do not make allowances for stiffener flexibilities that may exist in real panels with elastic boundary constraints. A different approach is to treat the buckled skin as orthotropic.[10,18] In Ref. 18, Van der Neut's work[19] on flat plate was extended to cover a post buckling biaxial stress field, so that the derived stiffness matrix can be used in the investigation of stiffened cylinders with buckled skin. Since a simple wave form of Koiter was used in Refs. 18 and 19 as the buckling pattern, it is speculated that more complete wave forms might yield different stiffness matrices. In fact, Stein[20] found that the shear stiffness of a buckled rectangular plate increases after a load ratio of 3, whereas Van der Neut's result showed that it continuously decreases. Improvement in this direction would be valuable.

In the buckling equation derived in Appendix B, two options for including the effect of locally buckled skin are

Table 1 Correlation of theories and tests for ring-stiffened corrugated cylinders

Cylinder number	R, in.	Frame spacing, in.	Load type[a]	Critical load from test, in.-lb. $\times 10^6$	Theory correlation (test/analysis)		
					Present analysis	Ref. 1[b]	Ref. 18[c]
NASA TN D-3336 (Ref. 1)							
2	38.84	13.3	B	2.30	0.92	0.86 0.68	
3	38.84	10.0	B	2.85	0.99	0.92 0.75	
4	38.84	8.0	B	3.10	0.96	0.92 0.75	
5	38.84	4.0	B	4.20	0.91	0.90 0.72	
NASA TN D-3089 (Ref. 9)							
1	24.7	6.38	A	131[d]	1.12		1.10
4	49.4	12.40	A	659[d]	1.05		1.00
6	197.6	51.00	C	334.8	0.98		1.04
7	24.7	6.38	B	1.932	0.95		

[a] A = uniform axial compression load, B = pure bending moment, and C = bending plus 6.93×10^6 lb axial compression load.
[b] Upper figures are predictions based on uniform axial compression analysis; lower figures are from bending theory. All data were taken from curves in the reference.
[c] Based on uniform compression analysis in predicting bending failure. Data were taken from curves in the reference.
[d] Critical load measured in pounds $\times 10^3$.

available. One is to treat the buckled skin as orthotropic. The stiffness matrix derived in Ref. 18 could be used as a first approximation. The other option is to extend Karman's idea of effective width,[15] as proposed by Boley[21] in his study of the reduction of shear stiffness in buckled curved plates, to cover in a gross manner the reductions of all stiffnesses of the buckled skin in strain energy expressions. Figure 3 shows a network of effective skin strips of variable width. In the buckling determinant, an exponential parameter from the effective width equation is chosen as a free parameter and its value is to be determined by correlating the predicted buckling stress with data from tests on a cylinder. Consequently,

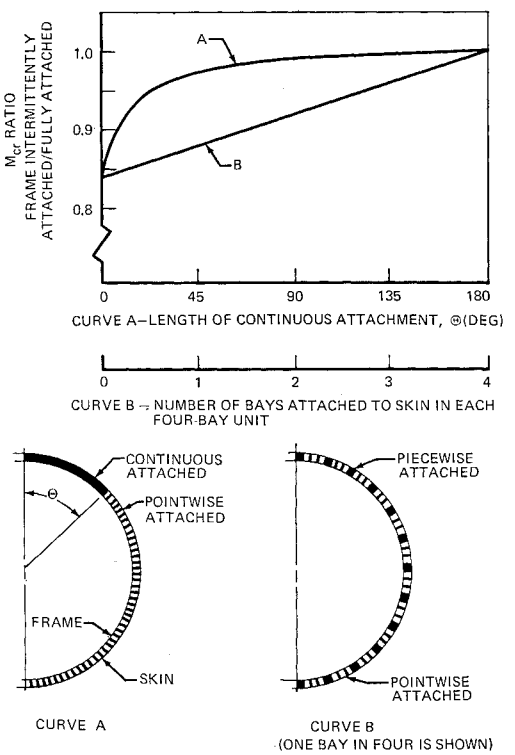

Fig. 4 Effect of length of frame-to-skin attachment on ring- and stringer-stiffened cylinders under bending moment with prematurely buckled skins.

errors due to simplifying assumptions in theory and idealization of structures are compensated for in an empirical manner. Calculations have indicated that if test data from one cylinder in a family are available to determine this effective width parameter, the predictions for other cylinders of comparable size and geometry are reasonably accurate and seem superior to some other methods.

V. Numerical Results and Correlations

A. Ring-Stiffened Corrugated Cylinders

The analysis was employed first to predict buckling of cylinders in which the stiffeners are monolithically attached to the skin. The orthotropic constants for corrugated sections are taken from Ref. 1. Table 1 shows the test data and predicted results from the present analysis and from Refs. 1 and 18 for eight large-diameter ring-stiffened corrugated cylinders from Refs. 1 and 9. It is to be noted that the curvature-displacement equations and the equilibrium equations for the stiffeners used in Ref. 18 are more exact than those used in the present analysis, but the quality of prediction of the two seems to be comparable.

Convergence of the results can be studied by increasing the terms of the displacement series of Eqs. (22). Assuming that the lateral deformation w is symmetric to the midplane of the cylinder, the wave numbers m are taken as from 1,3,5, . . ., 9 and the wave numbers n from 0,1,2, . . ., 14. The order of the determinant of Eq. (B5) is therefore 220 ($5 \times 15 + 5 \times 15 + 5 \times 14 = 220$). The convergence is checked by increasing the terms of the series from this basic pattern. For example, the results for cylinder 5 in Table 1 are given in Table 2. The convergence seems satisfactory.

B. Ring-and-Stringer Stiffened Cylinders

The analysis has also been correlated with results of a bending test from Card[10] in which six 77-in.-diam ring-and-stringer stiffened cylinders failed in general instability mode. Premature skin buckles were observed during the test. In using the effective width method of the present analysis, the required parameters $\bar{k}_2$ [Eq. (A3)] and q_s [Eq. (B17)] are first obtained from test data on an arbitrary cylinder (I-1 in group I) and analyses are then made for the rest of the cylinders based on the acquired parameter values. Table 3

Table 2 Check of convergence

Terms in Fourier series of w	Order of buckling determinant	M_{cr}, in.-lb
5 × 15	220	4.6446×10^6
5 × 16	235	4.6446×10^6
6 × 15	264	4.6441×10^6

shows the results based on Eq. (B5) and the predictions from Refs. 10 and 18, which predicted bending instability from analyses of uniform axial compression. The justification for such substitutions has been discussed in Ref. 22.

C. Effect of the Length of Frame-to-Skin Attachment

The effect of different lengths of frame-to-skin attachment on ring-and-stringer stiffened cylinders with prematurely buckled skin was calculated from a model cylinder (I-1 in Table 3) and is shown in Fig. 4. Assume that the frames are connected to the skin in a pointwise manner with a constant spacing that is the same as the spacing of the stringers (3.68°). The strength of such a cylinder is 83.5% of that of a corresponding cylinder with fully attached frames. Curve A shows the effect of changing the length of the continuously attached portion of frame and curve B shows the effect of distributing the length of attachment periodically around the circumference. From Fig. 4, one concludes that for equal lengths of frame-to-skin attachment, it is always superior, strengthwise, to use all attachment at the upper portion of the cylinder where the skin is in compression. In addition, the analysis shows that there is an optimum cutoff point on curve A, approximately at $\Theta = 45°$, at which further continuous connection seems not to improve the buckling strength.

D. Test Correlation with a Shear-Tied Floating-Type Cylinder

An important application for the present analysis is in the intermittently shear-tied, floating-type stiffened cylinders used widely as fuselages of large transport airplanes. A correlation with test results has been made, based on a recent test by The Boeing Company[17] to study the effect of addition of shear-ties on the bending instability strength of floating-type stiffened cylinders. The test specimen was an aluminum alloy half cylinder (like a Quonset hut) that had a radius of 127.75 in. and was 280-in. long. It was subjected to an axial compressive load that was zero at the diameter and increased linearly to the top. The straight sides of the half-cylinder specimen were clamped. The stringers, of standard hat section, 0.071-in. gage, 0.355-in.^{2} cross section, and 9.5-in. spacing, were riveted to the inside of the cylinder, which was of

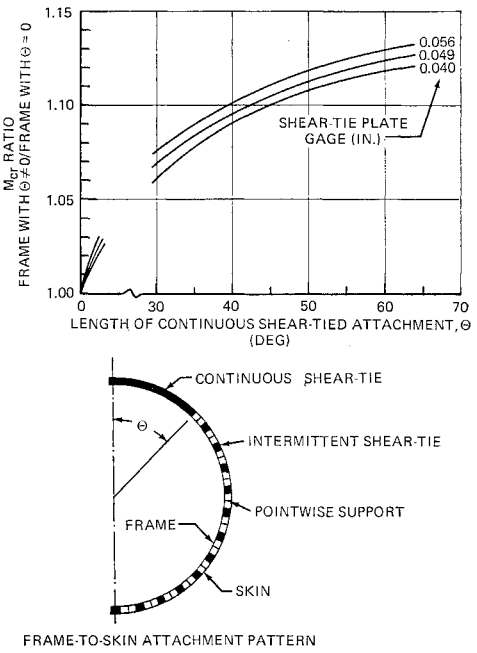

Fig. 5 Effect of shear-tied plate gage and length of continuously shear-tied attachment of frame of 128-in.-radius model.

0.080-in. skin gage. The frames had a gage of 0.056-in., cross-sectional area of 1.25 in.^{2}, and were of standard zee section with 20-in. spacing. The frames were connected to the stringers by standard clips. In the first test, the frames were shear tied (0.04-in. gage) at the top bay and then at every third bay, as shown in the sketch of Fig. 5. The test was nondestructive and a buckling crown compressive stress of 30,900 psi was indicated by extrapolations of load-deflection curves. The corresponding critical moment for a complete cylinder was calculated as 116.1×10^6 in.-lb. In the second test more shear ties were added to the upper portion of the previous test specimen such that the top quadrant (45° on both sides) of all frames was completely shear-tied to the skin; a sketch is shown in Fig. 5. The extrapolated buckling crown stress was 34,200 psi.

These tests showed that the additional attachment (plus the extra stiffness added to the frame by the shear-tie plates) of frames and skin had increased the critical crown stress by 10.7%. If the small difference between critical moment ratio and stress ratio is disregarded, the increment is very close to that indicated in Fig. 4. To predict the results of the second test, the two parameters $\bar{k}_2$ and q_s were calculated from data from the first test by Eqs. (A4–A6), and (B5). With $\bar{k}_2 = 0.4574$ and $q_s = 0.2854$, the predicted crown compressive

Table 3 Correlation of theories and tests[10] for ring-and-stringer stiffened cylinders with prematurely buckled skin

Cylinder number[a]	Frame spacing, in.	Test results: M_{cr}, in.-lb. × 10^6	Test results: σ_0, psi × 10^3	Theory correlations (test/analysis): Present analysis[c]: Value of $\bar{k}_2$[b]	Present analysis[c]: M_{cr}	Present analysis[c]: σ_0	Ref. 10[d]	Ref. 18[e]
I-1	6	5.32	43.5	0.292	1.00	1.00	1.04	0.95
I-2	9	4.68	37.0	0.27	0.99	0.97	1.03	0.89
I-3	12	4.44	35.0	0.27	1.02	1.00	1.05	0.87
II-1	6	3.40	41.0	0.32	0.99	1.03	1.19	1.09
II-2	9	3.05	36.0	0.30	1.03	1.04	1.19	1.08
II-3	12	2.88	34.0	0.31	1.07	1.10	1.21	1.11

[a] Cylinder radius = 38.6 in., test-section length = 72 in., hat-type internal frames and zee-type external stringers.
[b] Values were obtained from the test data for each cylinder [see Eq. (A3)].
[c] Based on $\bar{k}_2 = 0.292$ and $q_s = 0.189$, obtained from cylinder I-1.
[d] Predictions were based on analyses for uniform axial compression and taken from curve of M_{cr}.
[e] Predictions were based on analyses for uniform axial compression; correlation is based on load intensity N_x.

stress of the second test configuration was found to be 34,800 psi. Since the critical stress of the second test was obtained by extrapolation in a conservative manner, the error of prediction could have been less than 1.8%. It should be pointed out, however, that since the test specimen is an incomplete cylinder with clamped boundaries whereas the analysis is for a complete cylinder, the previous correlation should be viewed with caution.[22]

Figure 5 shows the results of an analytical study that involved changing the gage of the shear-tie plates and the length of the fully attached portion of the frames on a cylinder of the same construction as the Boeing test specimen. The results show again that 45° is a good cutoff point for addition of continuous shear-ties to the frames in the large, floating-type stiffened cylinders used in modern transport airplanes.

VI. Summary and Conclusions

An approximate analysis is derived for determining the general instability strength of stiffened cylinders with intermittently attached stiffeners. The technically important case of ring-and-stringer stiffened cylinders with prematurely buckled skin is studied in detail. Two options are available to account for the effect of the reduced stiffness of the buckled skin. If test results from a typical cylinder are available to establish the parameters $\bar{k}_2$ (which defines the relationship between the bending moment and the crown compressive stress) and q_s (which establishes the effective width in the sense of strain energy equivalence), the buckling strength of similarly constructed cylinders can be predicted with acceptable accuracy. For cylinders of comparable geometry to those described in Ref. 10, $\bar{k}_2 = 0.30$ and $q_s = q_r = 0.19$ might be used. For larger cylinders similar to the 128-in.-radius Boeing specimen,[17] $\bar{k}_2 = 0.457$ and $q_s = q_r = 0.285$ seem applicable. Otherwise, the buckled skin can be treated as orthotropic and the stiffness matrix suggested in Ref. 18 might be used in a first approximation estimate.

From the limited study reported here, one might conclude that the general instability strength of bending of ring-stiffened sandwich cylinders and ring-and-stringer stiffened isotropic cylinders with fully effective skin (these have been studied but the results are not elaborated here) is affected very little by decreasing the connections between frames and the skin of the cylinder. For ring-stiffened corrugated cylinders and ring-and-stringer stiffened cylinders with prematurely buckled skins, however, the bending buckling strength decreases as the frame-to-skin connection decreases. For those cylinders with prematurely buckled skins, continuous connection between frames and the skin for the top quadrant of the frame and then adequate discrete connections for the remainder of the frame have been found to be an optimum pattern that almost provides the full strength of a monolithic frame system.

Appendix A: Moment-Stress Relationships

If the skin buckles under a compressive load, the neutral axis of the cylinder section which is under bending moment will move toward the tension side. The relationship between the applied load and the compressive stress produced at the crown (where the compression is maximum) should be established.

The von Kármán effective width equation[15] associated with simply supported plate under uniaxial compression can be expressed as

$$W_e/d = [\bar{k}_1(t/d)^2(E/\sigma)]^{\bar{k}_2} \tag{A1}$$

where W_e is the effective width of the plate, d is the distance between the two supporting sides, σ is the local stress, $\bar{k}_2$ is a constant, and $\bar{k}_1 = k_1\pi^2/12(1-\nu^2)$, where k_1 is usually taken as 4.0.[23] Von Kármán suggested $\bar{k}_2 = \frac{1}{2}$ and Marguerre[24] used $\bar{k}^2 = \frac{1}{3}$.

If a plane section under bending is assumed to remain plane, the local stress at a point y on the midsurface of the skin of a cylinder can be expressed by

$$\sigma = \sigma_{xc} + \sigma_{xb} = \sigma_0(\cos y + h)/(1+h) \tag{A2}$$

where σ_{xc} and σ_{xb} are local stresses due to uniform axial compression and bending, respectively, σ_0 is the maximum compressive stress at the crown, and h is the nondimensional translation of the neutral axis.

Substitution of Eq. (A2) into (A1) yields

$$W_e/d = [\bar{k}_1(t/d)^2(E/\sigma_0)(1+h)/(\cos y + h)]^{\bar{k}_2} \tag{A3}$$

Since the effective width of a panel may not exceed its true width d, there is a maximum value of y, designated here as β, at which the skin starts to become less than fully effective. This angle β can be found from Eq. (A3) by putting $W_e = d$ and $y = \beta$. By so doing, one has

$$\cos\beta = \bar{k}_1(t/d)^2(E/\sigma_0)(1+h) - h \tag{A4}$$

It can be seen from Eq. (A4) that if $\beta = 0$, then $\sigma_0 = E \times (t/d)^2\bar{k}_1$, which is the maximum crown stress the cylinder can take without creating skin buckles.

Assuming the ith stringer is at $y = y_i$, the force and moment equilibrium equations of the section can be written, respectively, as

$$\frac{\sigma_0}{1+h}\left\{\sum_{i=1}^{y_i<\beta}(\cos y_i + h)\left(A_s + td\left[\frac{\bar{k}_1(t/d)^2E(1+h)}{\sigma_0(\cos y_i + h)}\right]^{\bar{k}_2}\right) + \sum_{i}^{\beta<y_i<\pi}(\cos y_i + h)A_s + \int_\beta^\pi(\cos y + h)tR\,dy\right\} = F_{xo} \tag{A5}$$

$$M_{cr} = \frac{2R\sigma_0}{1+h}\left\{\sum_{i=1}^{y_i<\beta}(\cos y_i + h)^2\left(A_s + td\times\left[\frac{\bar{k}_1(t/d)^2E(1+h)}{\sigma_0(\cos y_i + h)}\right]^{\bar{k}_2}\right) + \sum_{i}^{\beta<y_i<\pi}(\cos y_i + h)^2A_s + \int_\beta^\pi(\cos y + h)^2tR\,dy\right\} - F_{xo}hR \tag{A6}$$

where M_{cr} and F_{xo} are the applied moment and uniform compressive force, respectively. From Eqs. (A4) and (A5), the two unknown β and h can be expressed implicitly by σ_o. Substitutions of β and h into Eq. (A6) yields a relationship between the crown compressive stress σ_o and the applied load M_{cr} and F_{xo}.

Appendix B: Buckling Determinant

A buckling determinant for the general case of ring-and-stringer stiffened, orthotropic circular cylinders under bending and uniform axial compression is derived in this section. The effect of prematurely buckled skin is included. If the buckled homogeneous skin is treated as orthotropic material, its approximate stiffness matrix can be found from Ref. 18. A different method that often yields better results is presented here. It is assumed that a network of rectangular strips, as shown in Fig. 3, is substituted for the buckled panels of the shell, such that the elastic strain energies in the strips due to buckling deformations are equal to the actual change in strain energy of the buckled skin of the cylinder. Thus, the ith stringer supports a strip of skin of width $\bar{W}_s(i)$ from $x = 0$ to L, and the frame, if it is continuously attached to the skin at $y = y_i$, could also support an effective strip of width $\bar{W}_r(i)$.

Thus, Eq. (1) can be rewritten as

$$U_c/R^2 = \int_0^L \int_\beta^\pi [A_1(u_{,x})^2 + \ldots A_8(w_{,yy})^2]dxdy + \sum_{i=1}^{y_i<\beta} \int_0^L \int_{y_i-(\frac{1}{2})\bar{W}_s(i)}^{y_i+(\frac{1}{2})\bar{W}_s(i)} [A_1(u_{,x})^2 + .. \ldots A_8(w_{,yy})^2]dxdy + \sum_{j=1}^{0<x_j<L} \sum_{i}^{y_i<\beta} \int_{x_j-(\frac{1}{2})\bar{W}r(i)}^{x_j+(\frac{1}{2})\bar{W}r(i)} \int_{y_{i-1}+(\frac{1}{2})\bar{W}_s(i-1)}^{y_i-(\frac{1}{2})\bar{W}_s(i)} [A_1(u_{,x})^2 + \ldots]dxdy \quad \text{(B1)}$$

The potential of the loads, Eqs. (20) and (21), shall be rewritten as

$$U_{p(\text{skin})} = -\frac{\sigma_0}{1+h}\left\{R \sum_{i=1}^{y_i<\beta} \int_0^L (\cos y_i + h)td \times \left[\frac{\bar{k}_1(t/d)^2E(1+h)}{\sigma_0(\cos y_i + h)}\right]^{\bar{k}_2} (w_{,x}|_{y=y_i})^2\, dx + R^2 \int_0^L \int_\beta^\pi (\cos y + h)\, t\, (w_{,x})^2 dxdy\right\} \quad \text{(B2)}$$

$$U_{p(\text{stringers})} = -\sum_{i=1}^{y_i<\pi} \int_0^L R\sigma_0 \frac{(\cos y_i + h)}{1+h} A_s(w_{,x}|_{y=y_i})^2 dx \quad \text{(B3)}$$

The buckling determinant can be found as in the following. Let U be the sum of the changes of the elastic strain energies of the structure as expressed in Eqs. (B1, 4, 6, and 15, and of the potential of the load as expressed in Eqs. (B2) and B3). By substitution of the symmetric buckling mode expressed by Eqs. (22) into the total potential U and differentiation with respect to the coefficients $W_{m'n'}(m' = 1, 2, \ldots, \infty; n' = 0, 1, \ldots, \infty)$, $U_{m'n'}(m' = 1, 2, \ldots, \infty; n' = 0, 1, \ldots, \infty)$, and $V_{m'n'}$ $(m' = 1, 2, \ldots, \infty; n' = 1, 2, \ldots, \infty)$, one obtains the following linear homogeneous equations:

$$\begin{Bmatrix} \partial(U/R^2L)/\partial W_{m'n'} \\ \partial(U/R^2L)/\partial U_{m'n'} \\ \partial(U/R^2L)/\partial V_{m'n'} \end{Bmatrix} = \sum_{m=1}^{\infty}\left(\sum_{n=0}^{\infty} W_{mn}\begin{Bmatrix} E_{11} \\ E_{21} \\ E_{31} \end{Bmatrix} + \sum_{n=0}^{\infty} U_{mn}\begin{Bmatrix} E_{12} \\ E_{22} \\ E_{32} \end{Bmatrix} + \sum_{n=1}^{\infty} V_{mn}\begin{Bmatrix} E_{13} \\ E_{23} \\ E_{33} \end{Bmatrix}\right) = 0 \quad \text{(B4)}$$

The associated buckling determinant can be written as

$$\begin{vmatrix} E_{11} & E_{12} & E_{13} \\ E_{21} & E_{22} & E_{23} \\ E_{31} & E_{32} & E_{33} \end{vmatrix} = 0 \quad \text{(B5)}$$

where the E elements are functions of the indices m' and n', which determine its row position in the determinant, and of m and n, which determine its column position. These elements are given in the following:

$$E_{11} = [A_4 + A_5\bar{m}^2\bar{m}'^2 + A_6(\bar{m}^2n'^2 + \bar{m}'^2n^2) + A_8n^2n'^2]\Omega_1 + \bar{m}'n\bar{m}n'A_7\Omega_2 + \delta_{mm'}\left\{\sum_{i=1,2}^{0<y_i<\pi} (\bar{m}^4A_{11}\cos ny_i \cos n'y_i + \bar{m}^2nn'A_{12}\sin ny_i \sin n'y_i)\right\} + (2/L)\left\{\sum_{j=1,2}^{0<x_j<L}\sum_{i=1,2}^{0<y_i<\pi} \times \Phi_{ji}(1)\right\} - \frac{\sigma_0\delta mm'\bar{m}^2}{(1+h)R}\left\{\sum_{i=1}^{0<y_i<\beta} td\left[\frac{\bar{k}_1(t/d)^2E(1+h)}{\sigma_0(\cos y_i + h)}\right]^{\bar{k}_2} \times (\cos y_i + h)\cos ny_i\cos n'y_i + \int_\beta^\pi Rt(\cos y + h)\cos ny \cos n'ydy + \sum_{i=1,2}^{0<y_i<\pi} A_s(\cos y_i + h)\cos ny_i \cos n'y_i\right\} \quad \text{(B6)}$$

$$\begin{Bmatrix} E_{12} \\ E_{22} \\ E_{23} \end{Bmatrix} = \begin{Bmatrix} \bar{m}A_2 \\ \bar{m}'\bar{m}A_1 \\ -\bar{m}'nA_2 \end{Bmatrix}\Omega_1 + \begin{Bmatrix} 0 \\ n'nA_3 \\ -\bar{m}'n'A_3 \end{Bmatrix}\Omega_2 + \delta mm' \times \sum_{i=1,2}^{0<y_i<\pi} \begin{Bmatrix} -A_{10}\bar{m}^3 \\ A_9\bar{m}^2 \\ 0 \end{Bmatrix} \cos ny_i \cos n'y_i \quad \text{(B7)}$$

$$\begin{Bmatrix} E_{13} \\ E_{33} \end{Bmatrix} = \begin{Bmatrix} -nA_4 \\ n'nA_4 \end{Bmatrix}\Omega_1 + \begin{Bmatrix} 0 \\ \bar{m}'\bar{m}A_3 \end{Bmatrix}\Omega_2 + (2/L) \times \sum_{j=1,2}^{0<x_j<L}\sum_{i=1,2}^{0<y_i<\pi} \begin{Bmatrix} \Phi_{ji}^{(2)} \\ \Phi_{ji}^{(3)} \end{Bmatrix} \quad \text{(B8)}$$

where $\delta_{mm'}$ is the usual Kronecker delta function which is equal to unity when $m = m'$ and which vanishes when $m \neq m'$, and Ω_1, Ω_2 are given by

$$\begin{Bmatrix} \Omega_1 \\ \Omega_2 \end{Bmatrix} = \delta_{mm'}\left[\sum_{i=1,2}^{0<y_i<\beta} \int_{y_i-(\frac{1}{2})\bar{W}_s(i)}^{y_i+(\frac{1}{2})\bar{W}_s(i)} \begin{Bmatrix} \cos ny \cos n'y \\ \sin ny \sin n'y \end{Bmatrix} dy + \int_\beta^\pi \begin{Bmatrix} \cos ny \cos n'y \\ \sin ny \sin n'y \end{Bmatrix} dy\right] + (2/L)\sum_{j=1,2}^{0<x_j<L}\sum_{i=1,2}^{0<y_i<\beta} \begin{Bmatrix} \psi_1 \\ \psi_2 \end{Bmatrix} \quad \text{(B9)}$$

where

$$\begin{Bmatrix} \psi_1 \\ \psi_1 \end{Bmatrix} = \int_{x_j-(\frac{1}{2})\bar{W}r(i)}^{x_j+(\frac{1}{2})\bar{W}r(i)} \int_{y_{i-1}+(\frac{1}{2})\bar{W}_s(i-1)}^{y_i-(\frac{1}{2})\bar{W}_s(i)} \times \begin{Bmatrix} \sin\bar{m}x \sin\bar{m}'x \cos ny \cos n'y \\ \cos\bar{m}x \cos\bar{m}'x \sin ny \sin n'y \end{Bmatrix} dxdy \quad \text{(B10)}$$

if the jth frame is continuously attached to the skin between y_{i-1} and y_i and $= 0$ if the jth frame is not attached between y_{i-1} and y_i.

The quantities $\Phi_{ji}^{(1)}$, $\Phi_{ji}^{(2)}$, and $\Phi_{ji}^{(3)}$ shown in Eqs. (B6) and (B8) are functions of the frame location. Their values depend on whether the frame is attached to the skin or not. If the jth frame (at $x = x_j$) is continuously attached to the skin between y_{i-1} and y_i, then

$$\Phi_{ji}^{(1)} = \sin\bar{m}x_j \sin\bar{m}'x_j[B_1 - B_2(n^2 + n'^2) + B_3n^2n'^2]\int_{y_{i-1}}^{y_i} \times \cos ny \cos n'ydy + \cos\bar{m}x_j \cos\bar{m}'x_j\, B_4\bar{m}\bar{m}'nn' \int_{y_{i-1}}^{y_i} \times \sin ny \sin n'ydy \quad \text{(B11)}$$

$$\begin{Bmatrix} \Phi_{ji}^{(2)} \\ \Phi_{ji}^{(3)} \end{Bmatrix} = \begin{Bmatrix} (-nB_1 + n'^2nB_2) \\ n'nB_1 \end{Bmatrix} \sin\bar{m}x_j \sin\bar{m}'x_j \times \int_{y_{i-1}}^{y_i} \cos ny \cos n'ydy \quad \text{(B12)}$$

Otherwise, they are defined as

$$\Phi_{ji}^{(1)} = K_1\{Q_1(n,i)[G_1\cdot Q_1(n',i) + G_5\cdot Q_2(n',i) + G_6\cdot Q_3(n',i)] + Q_2(n,i)[G_5\cdot Q_1(n',i)] + G_2\cdot Q_2(n',i) + G_4\cdot Q_3(n',i)] + Q_3(n,i)[G_6\cdot Q_1(n',i) + G_4\cdot Q_2(n',i) + G_3\cdot Q_3(n',i)]\} + (K_1/R)\cos\bar{m}x_j \cos\bar{m}'x_j\, G_7\bar{m}\bar{m}'(\cos ny_i - \cos ny_{i-1})(\cos n'y_i - \cos n'y_{i-1}) \quad \text{(B13)}$$

$$\begin{Bmatrix}\Phi_{ji}^{(2)}\\ \phi_{ji}^{(3)}\end{Bmatrix} = (K_1/R)\sin\bar{m}x_j \sin\bar{m}'x_j \left(Q_4(n,i)\left[G_1\begin{Bmatrix}Q_1(n',i)\\ Q_4(n',i)\end{Bmatrix} + G_5\begin{Bmatrix}Q_2(n',i)\\ Q_5(n',i)\end{Bmatrix} + G_6\begin{Bmatrix}Q_3(n',i)\\ Q_6(n',i)\end{Bmatrix}\right] + Q_5(n,i)\left[G_5\begin{Bmatrix}Q_1(n',i)\\ Q_4(n',i)\end{Bmatrix} + G_2\begin{Bmatrix}Q_2(n',i)\\ Q_5(n',i)\end{Bmatrix} + G_4\begin{Bmatrix}Q_3(n',i)\\ Q_6(n',i)\end{Bmatrix}\right] + Q_6(n,i)\left[G_6\begin{Bmatrix}Q_1(n',i)\\ Q_4(n',i)\end{Bmatrix} + G_4\begin{Bmatrix}Q_2(n',i)\\ Q_5(n',i)\end{Bmatrix} + G_3\begin{Bmatrix}Q_3(n',i)\\ Q_6(n',i)\end{Bmatrix}\right]\right) \quad \text{(B14)}$$

where G_1, Q_1, etc. are given in Eqs. (16) and (24), respectively. It is to be noted that m', first seen in Eq. (B10), is defined the same as m in the Nomenclature except that m is replaced by m'. Similarly, $Q_1(n',i)$ is defined the same as $Q_1(n,i)$ in Eqs. (24) except that n is replaced by n'.

The remaining elements E_{21}, E_{31}, and E_{32} are the transposes of E_{12}, E_{13}, and E_{23}, respectively; that is, the determinant as expressed by Eq. (B5) is symmetric to the diagonal.

The buckling stress σ_0 at the crown is the smallest positive eigenvalue σ_0 of Eq. (B5) and it can be solved numerically in a digital computer.

Finally, the expressions of the effective width, $\bar{W}_s(i)$ and $\bar{W}_r(i)$, remain to be determined. Similar to von Kármán's equation in Eq. (A3), the nondimensional width of skin associated with the ith stringer will be expressed as

$$\bar{W}_s(i) = (d/R)[\bar{k}_1(t/d)^{q_f}(E/\sigma_0)(1+h)/(\cos y_i + h)]^{q_s} \quad \text{(B15)}$$

where two new constants q_f and q_s are introduced. The width $\bar{W}_r(i)$ associated with the attached frame at ith bay is given by

$$\bar{W}_r(i) = (d/R)[\bar{k}_1(t/d)^{q_f}(E/\sigma_0)(1+h)/(\cos y_{i-1} + h)]^{q_r} \quad \text{(B16)}$$

As a first approximation, q_r is assumed to be the same as q_s; then $\bar{W}_r(i+1) = \bar{W}_s(i)$ and there are only two unknown parameters q_f and q_s to be determined. Since these parameters are meant to compensate for the discrepancies of the idealizations made to simplify the flexible stiffener-skin assembly to the simply supported flat plates, their values should be determined from test data. Based on the six large cylinder bending tests by Card,[10] one may choose arbitrarily two cylinders, I-1 and II-2 in Table 3, and establish a relationship between q_f and q_s from the test data of M_{cr} and σ_0 of the two cylinders. At $q_f = 3.3$, the two curves almost cross each other; thus, by substitution of $q_f = 3.3$ and $\bar{k}_1 = \pi^2/3 \times (1-\nu^2)$, Eqs. (B15) and (B16) yield

$$\bar{W}_s(i) = \bar{W}_r(i+1) = (d/R)\{[\pi^2/3(1-\nu^2)](t/d)^{3.3}(E/\sigma_0) \times (1+h)/(\cos y_i + h)\}^{q_s} \quad \text{(B17)}$$

Equation (B17) will be used in Eq. (B5) for large-diameter cylinders with geometry similar to the specimens in Ref. 10 where zee sections were used for stringers and hat sections for frames. For approximate estimations, it may also be used for large cylinders with comparable stiffeners. If the skin is treated as orthotropic, $\bar{W}_s$ and $\bar{W}_r$ should be made equal to the spacings of the stringers and frames, respectively, in Eq. (B1), which then is reduced to the original Eq. (1).

It is to be noted that since stringers are treated as discrete members and effective skin widths are integrated numerically in Eqs. (B1–B3), the present analysis is applicable to cylinders with variable stringers and skin gages that change moderately with the circumferential coordinate.

References

[1] Peterson, J. P. and Anderson, J. K., "Bending Tests of Large-Diameter Ring-Stiffened Corrugated Cylinders," TN D-3336, March 1966, NASA.

[2] Anderson, J. K., "Bending Tests of Two Large-Diameter Corrugated Cylinders With Eccentric Ring Stiffeners," TN D-3702, Nov. 1966, NASA.

[3] Baruch, M. and Singer, J., "The Effect of Eccentricity on the General Instability of Stiffened Cylindrical Shells Under Hydrostatic Pressure," *Journal of Mechanical Engineering Sciences*, Vol. 5, No. 1, March 1963, pp. 23–27.

[4] Singer, J. and Haftka, R., "Buckling of Discretely Ring Stiffened Cylindrical Shells," TAE Rept. 67, Aug. 1967, Technion, Israel Institute of Technology, Haifa, Israel.

[5] Gerard, G., "Elastic and Plastic Stability of Orthotropic Cylinders," TN D-1510, *Collected Papers on Instability of Shell Structures—1962*, Dec. 1962, NASA, p. 277.

[6] Becker, H., Gerard, G., and Winter, R., "Experiments on Axial Compressive General Instability of Monolithic Ring-Stiffened Cylinders," *AIAA Journal*, Vol. 1, No. 7, July 1963, pp. 1614–1618.

[7] Card, M. F., "Preliminary Results of Compression Tests on Cylinders with Eccentric Longitudinal Stiffeners," TM X-1004, Sept. 1964, NASA.

[8] Meyer, R. R., "Buckling of 45° Eccentric Stiffened Waffle Cylinders," *Journal of Royal Aeronautical Society*, Vol. 71, July 1967, p. 516.

[9] Dickson, J. N. and Brolliar, R. H., "The General Instability of Ring-Stiffened Corrugated Cylinders Under Axial Compression," TN D-3089, Jan. 1966, NASA.

[10] Card, M. F., "Bending Tests of Large-Diameter Stiffened Cylinders Susceptible to General Instability," TN D-2200, April 1964, NASA.

[11] Singer, J., "The Influence of Stiffener Geometry and Spacing on the Buckling of Axially Compressed Cylindrical and Conical Shells," *IUTAM Symposium, Copenhagen 1967*, edited by F. I. Niordson, Springer-Verlag, Berlin, 1969.

[12] Block, D. L., Card, M. F., and Mikulas, M. M., "Buckling of Eccentrically Stiffened Orthotropic Cylinders," TN D-2960, Aug. 1965, NASA.

[13] Stein, M. and Mayers, J., "A Small Deflection Theory for Curved Sandwich Plates," Rept. 1008, 1951, NACA.

[14] Soong, T. C., "Buckling of Cylindrical Shells with Eccentric Spiral-Type Stiffeners," *AIAA Journal*, Vol. 7, No. 1, Jan. 1969, pp. 65–72.

[15] von Kármán, T., Sechler, E. E., and Donnell, L. H., "The Strength of Thin Plates in Compression," *Transactions of the ASME*, Vol. 54, 1932, p. 53.

[16] "Some Investigations of the General Instability of Stiffened Metal Cylinders: V-Stiffened Metal Cylinders Subjected to Pure Bending," TN 909, 1943, NACA.

[17] Salisbury, G. A., "Group Report T6-4090-Informal, Report No. 16, Structures Laboratory—Structural Test Group," Sept. 1968, The Boeing Company, Seattle, Wash.

[18] Dickson, J. N. and Brolliar, R. H., "The General Instability of Eccentrically Stiffened Cylindrical Shells Under Axial Compression and Lateral Pressure," CR-1280, Jan. 1969, NASA.

[19] Van der Neut, A., "The Post-Buckling Stiffness of Rectangular Simply Supported Plates," Rept. VTH-113, Oct. 1962, Technische Hogeschool, Delft, Netherlands.

[20] Stein, M., "Behavior of Buckled Rectangular Plates," *Journal of the Engineering Mechanics Division, ASCE*, April 1960, pp. 59–76.

[21] Boley, B. A., "The Shearing Rigidity of Buckled Sheet Panels," *Journal of the Aeronautical Sciences*, Vol. 17, No. 6, June 1950, pp. 356–362.

[22] Soong, T. C., "Reply by Author to R. R. Meyer," *AIAA Journal*, Vol. 7, No. 10, Oct. 1969, pp. 2047–2048.

[23] Timoshenko, S. and Gere, J. M., *Theory of Elastic Stability*, 2nd ed., McGraw-Hill, New York, 1964, p. 355.

[24] Marguerre, K., "Die mittragende Breite der gedruckten Platte," *Luftfahrtforschung*, Vol. 14, 1937, p. 121.